Strain-induced modulation versus superlattice ordering in epitaxial (GaIn)P layers

Jiechao Jiang,* Andreas K. Schaper,† Zeljko Spika,‡ and Wolfgang Stolz
Materials Science Center, Philipps University Marburg, Hans-Meerwein-Strasse, 35032 Marburg, Germany
(Received 7 December 1999; revised manuscript received 18 May 2000)

One main goal of the present work was to perform specific metal-organic vapor-phase epitaxy experiments to prove existing models for the fundamental process of superlattice ordering in the model system (GaIn)P. Applying a modulated-growth regime, we prepared (GaIn)P/GaAs multilayers, which enabled us to follow the structural and morphological development in dependence on the deposition cycle of the constituent binary components by transmission electron microscopy and electron diffraction investigations. The thickness of the alternating deposition layers was varied in the range $0.40 \leqslant n \leqslant 1.66$. From the systematic investigations we could gain new insight into the mechanisms of the reconstruction of group-V stabilized growth surfaces and of the general role surface reconstruction processes play in CuPt superlattice ordering. A competitive interaction was revealed between the mechanisms of ordering and processes that lead to morphological and compositional modulation structures. The lattice mismatch of the constituent binary alloys and the accumulation of the misfit strains is suggested as the main driving force for the modulation. Those self-organization capabilities of strained epitaxial layers are of considerable interest in view of low-dimensional confinement formations.

I. INTRODUCTION

Spontaneous ordering on atomic and mesoscopic scales in the epitaxy of ternary and quaternary semiconductor alloys has attracted increasing interest with current efforts in the development of high-performance systems for novel device applications. It has become clear that systematic deviations from the atomically disordered state may greatly alter the optical properties of the materials due to band-gap narrowing as well as valence-band splitting.[1–5] On the other hand, much attention is paid now to self-assembly systems for fabricating low-dimensional structures that show quantum-confinement effects. Strain-induced lateral ordering and composition modulation seem very promising to realize this type of functional layer.[6–11]

Since the work of Suzuki and co-workers,[12–14] the tendency of (GaIn)P to show chemical ordering of the group-III atoms on {111} lattice planes forming a CuPt-type structure has been well-established. Recently, detailed theoretical approaches have led to the conclusion that surface reconstruction plays a predominant role in the ordering formation process.[15–20] The driving force for this kind of superlattice ordering comes from the dimerization of the surface phosphorus atoms and the formation of crystallographically oriented dimer rows on the growing surface. The most probable reconstruction modes proposed are the $c(2\times4)$ reconstruction with the 2×1 motif of a model surface, and the $c(4\times4)$ reconstruction with the basic 1×2 motif.[20] While the former stabilizes the two $CuPt_B$ variants of ordering parallel to the $(111)B$ steps, the latter should cause $CuPt_A$ ordering.[19] Until now, the A type of ordering has been discovered in (AlIn)P only.[21]

The development of CuPt superlattice ordering is basically controlled by the growth conditions[22–28] such as growth temperature, growth rate, and V/III ratio and by the misorientation of the substrate.[14,27,29–32] Recently, we have reported the application of a modulation scheme during metal-organic vapor phase epitaxy (MOVPE) of (GaIn)P on GaAs that allows further to improve the degree of ordering as compared to conventional growth methods.[33] The modulated growth consists in an alternating deposition of each binary component of the alloy with precise adjustment of the deposition rate and cycle time by controlling the constituent gas streams of the gallium and indium sources at continuous phosphorus source flux. Due to the continuous supply of phosphorus, the growing surface remains always under P-stabilized reconstruction conditions throughout the epitaxial layer growth.

From previous investigations we know that, besides the well-known platelike antiphase domains, under modulated MOVPE conditions a columnar domain morphology is formed[33,34] that originates from a two-dimensional structure modulation. Spontaneous large-scale ordering due to the phase separation over many tens of lattice spacings has so far been known among the ternary-alloy systems, primarily from gas-source molecular beam epitaxy (MBE) of short-period superlattices (SPS) of $(GaP)_n/(InP)_m$ on GaAs,[6,35–37] $(InAs)_n/(GaAs)_m$ on InP,[6] and $(AlAs)_n/(InAs)_m$ on InP for $n \cong m \cong 2$,[10,38–42] and from MBE of (GaIn)As on InP with varying In/Ga ratio.[43] Similar quasiperiodic composition variations were observed in quaternary systems like (GaIn)(AsP) on InP grown by liquid-phase epitaxy (LPE).[44–47] As far as well-matched MOVPE-grown (GaIn)P bulk layers are concerned, there are, however, only a few observations reported in the literature of spinodal-like decomposition until now.[48,49]

Continuous-wave and time-resolved optical spectroscopy measurements have shown us that the complex modulation morphology changes the time scale of the exciton relaxation and determines their recombination path.[50] Using scanning near-field optical microscopy, spatially resolved photoluminescence (PL) experiments have indicated the dependence of the optical properties from the local environment within the layers.[51] To improve our understanding of the structure/property relationships of those systems, in the present work we have studied the onset and the evolution of the structural

organization on different length scales in modulated MOVPE-grown (GaIn)P using particular double-multilayer samples. By means of systematic variation of the thickness of the elementary monolayers (ML's) within such a multilayer system we were able to control the superlattice ordering and to gain new insight into the mechanisms of the ordering process. Our attention has further focused on the competing formation of a strain-induced two-dimensional modulation morphology that transforms into a three-dimensional (3D) Stranski-Krastanov mode at monolayer thicknesses $n > 1.7$. The latter, however, is not subject of this study.

II. MATERIALS AND METHODS

The epitaxy experiments were carried out in a horizontal MOVPE reactor (Aix 200, Aixtron) using trimethylgallium (TMGa), trimethylindium (TMIn), and phosphine (PH_3) as source materials in a hydrogen carrier gas. The reactor pressure was 100 mbar at a V/III ratio of 60. A growth rate of 1.1 μm/h was chosen, and the samples were rotated on a hydrogen gas foil cushion during growth. Before growth of the epilayers, a 100 nm thick buffer layer was deposited on the GaAs substrate to minimize any substrate effects. On (001) GaAs substrates with a misorientation of 4° and 5° in the $[1\bar{1}0]$ direction we prepared multiple GaAs/(GaIn)P double-layer structures. The (GaIn)P layers of approximately 180 nm thickness were deposited in an alternating sequence with 40 nm thin GaAs intermediate layers. The modulated growth was performed under P-stabilized conditions at an alternating deposition of n monolayers of GaP and n monolayers of InP per deposition cycle. The cycle period was systematically changed from one epitaxial (GaIn)P superlayer to the other so as to vary the elementary layer thickness within one and the same sample in the range $0.40 \leqslant n \leqslant 1.70$ monolayers. Figure 1 schematically illustrates a section of such a multiple double-layer structure prepared face-to-face for transmission electron microscopy (TEM).

The CuPt ordering within each (GaIn)P layer was quantified utilizing the fact that, in the case of a kinematical approach, the intensity scattered into a superlattice reflection is proportional to the amount of ordering weighted by the average structure factor of the alloy.[52,53] Selected-area transmission electron diffraction (TED) zinc blende patterns were taken from layer regions near the inner edge of the specimen along an imaginary circular line that represents identical sample thicknesses. Hence, the influence of dynamic effects onto the diffraction intensities is minimized. The TED patterns were acquired from negatives using a charge-coupled device (CCD) camera, and were calibrated by means of a Kodak gray-scale calibration strip of known optical densities. Analysis of the scattering intensity of a superspot, e.g., of the $\frac{1}{2}(1\bar{1}1)$ reflection, was accomplished in relation to the intensity of the corresponding fundamental reflection of the zinc-blende structure.

In addition, bulk (GaIn)P mixed crystals of ~ 1.5 μm total thickness were deposited under modulated MOVPE conditions with $n \leqslant 1$ ML on substrates with orientations of exactly (001), 4°, and 5° off cut. A growth temperature of 650 °C was used, and the applied growth rates ranged from 0.66 to 1.35 μm/h. The degree of ordering in these layers

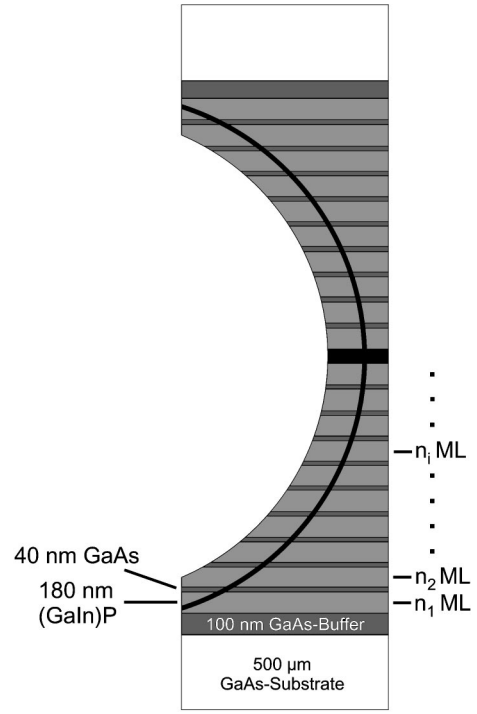

FIG. 1. Schematic drawing of a cross-sectional sample of a multiple-double-layer structure of (GaIn)P/GaAs after preparation for TEM. Electron-diffraction analysis was accomplished along the dark circular line inserted, indicating locations of constant sample thickness. For further details see text.

was estimated from the reduction in band-gap energy[3] applying photoluminescence spectroscopy. Correction of the PL spectra was done in terms of the thermal distribution of the charge carriers at room temperature over the density of states, which shifts the energy maximum by $\Delta E = +k_B T/2$.

Thinning of the samples for TEM occurred by Ar-ion milling in a Gatan DuoMill, the TEM investigations were performed using a Philips CM 20 operating at 200 kV, and a JEOL JEM 4000EX operating at 400 kV. Microanalytical measurements were accomplished using a VG HB-501UX scanning transmission electron microscope at 100 kV equipped with an energy-dispersive x-ray (EDX) spectrometer with a Ge detector (Noran Instruments).

III. RESULTS

The epitaxial growth of (GaIn)P/GaAs multilayer structures with systematically varied ML thicknesses and the preparation of these multilayers for TEM were the essential experimental requirements for the following measurements. The dark-field electron micrographs using the $\frac{1}{2}(1\bar{1}1)$ superlattice spot along with the corresponding selected-area diffraction patterns in Fig. 2 show, as an example for the case of growth on a substrate with 5° off-cut, the results of one specimen including eight (GaIn)P layers with gradually increasing ML thickness during modulated MOVPE starting from $n = 0.40$ up to $n = 1.44$. The diffraction pattern of each single epilayer corresponds to a region of less than 100 nm diameter and was taken at an almost equal distance from the

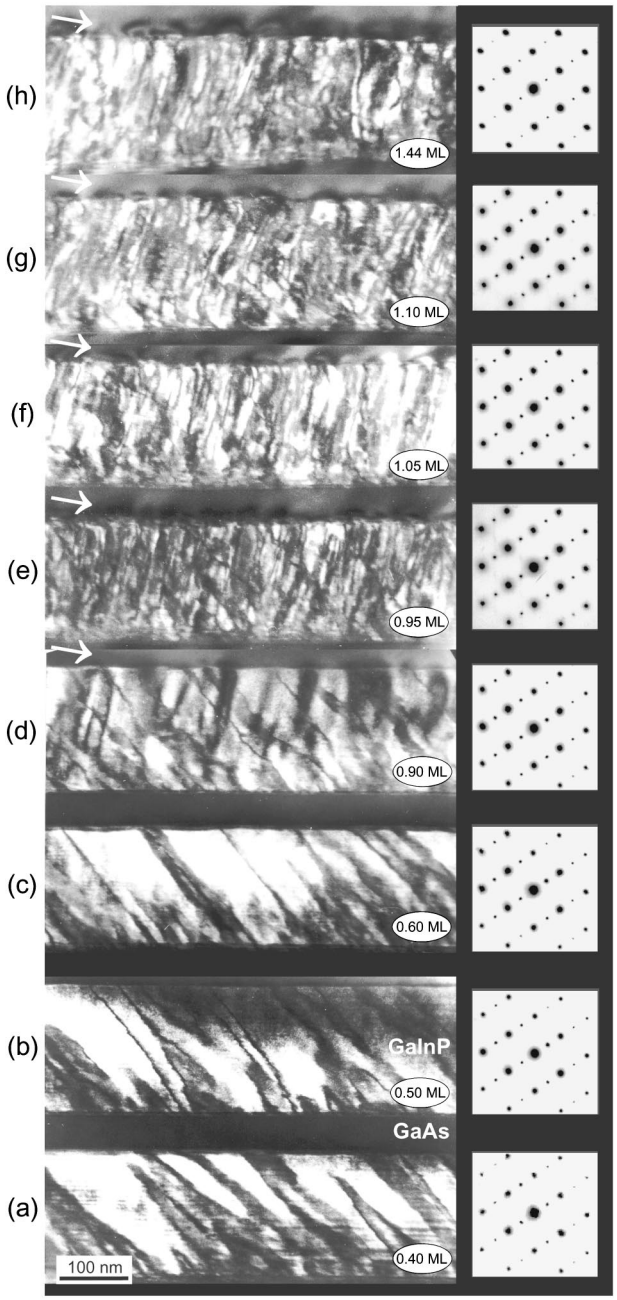

FIG. 2. $\frac{1}{2}(1\bar{1}\bar{1})$ dark-field electron micrographs and corresponding selected-area diffraction patterns of (110) cross sections of (GaIn)P layers with increasing individual layer thickness of a multilayer structure modulation-grown at 650 °C on 5° misoriented GaAs: (a) 0.40 ML, (b) 0.50 ML, (c) 0.60 ML, (d) 0.90 ML, (e) 0.95 ML, (f) 1.00 ML, (g) 1.10 ML, (h) 1.44 ML. The TED patterns were taken from a region of approximately 100 nm diameter in each case. The arrows point the array of strain-induced contrast contours inside the GaAs intermediate layers in direct relation to the columnar domains in the (Ga, In)P epilayers.

inner edge of the sample hole. The degree of local order was quantified by estimating the ratio of the scattering intensity in the $\frac{1}{2}(1\bar{1}\bar{1})$ ordering reflection and the intensity of the main {111} zinc-blende lattice spot. (The intensity variations of the diffraction spots in Fig. 2 are hardly detected by the naked eye.)

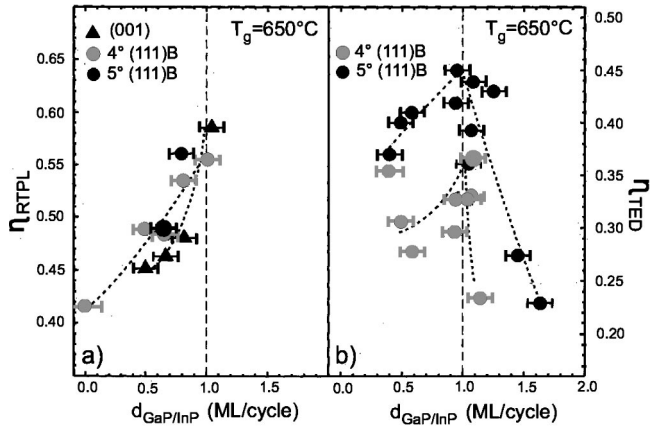

FIG. 3. Photoluminescence and transmission electron diffraction derived ordering parameter in dependence on the monolayer thickness per deposition cycle of bulk and multiple layers, respectively. The measures are for different substrate cutoffs at a growth temperature of 650 °C.

The results of the evaluation of series of electron-diffraction patterns from several multilayer structures are plotted in Fig. 3 together with the ordering parameter derived by room-temperature photoluminescence (RTPL) measurements. While the RTPL data, obtained using bulk epilayers at exact substrate orientation and at 4° and 5° misorientation hold for layer thicknesses n up to 1 ML GaP/InP per deposition cycle, the TED data cover a range $0.40 \leqslant n \leqslant 1.66$ ML for 4° and 5° off-cuts, respectively. Both the optical and the structural ordering parameters η_{RTPL} and η_{TED} show the same tendency to steadily increase with increasing individual layer thickness up to $n \approx 1$ ML. Beyond this region, the opposite trend in the ordering behavior is detected as clearly revealed by the continuous decrease in η_{TED}. The maximum ordering parameters of 0.58 in the RT PL analysis and of 0.45 in the TED analysis correspond to 300 K band-gap energies of about 1.74 eV (exact orientation) and 1.79 eV (5° off orientation), respectively. These are, to our knowledge, among the lowest values reported in the literature along with the band gap of 1.78 eV dealt with for atomic layer epitaxy (ALE) grown (GaIn)P.[54] Although the determination of the degree of ordering by TED has led to smaller values as compared to the PL measurements, the dependence on the modulation conditions is unambiguously established by both methods. The differences in the results are presumably caused by the inappropriate specimen thicknesses at the location from where the TED patterns were taken, i.e., by dynamic effects in the scattering experiments, and by the differing domain sizes within the samples studied. This may also apply for the differences in the η_{TED} values for the two different substrate misorientations. There are other results that show, under modulated growth conditions at 650 °C and using the same growth rate, that the influence of the misorientation of the substrate on the final degree of ordering is neglegible.[33,55]

The sequence of the dark-field images in Fig. 2, viewed along the [110] direction, shows a typical antiphase domain structure which, beginning at about 0.9 ML, becomes superimposed by contrast modulations crossing the antiphase domains at an inclination of usually less than 10° against the layer normal within the (110) plane. At $n = 0.9$ ML, the modulation contrast appears for the first time about 100 nm

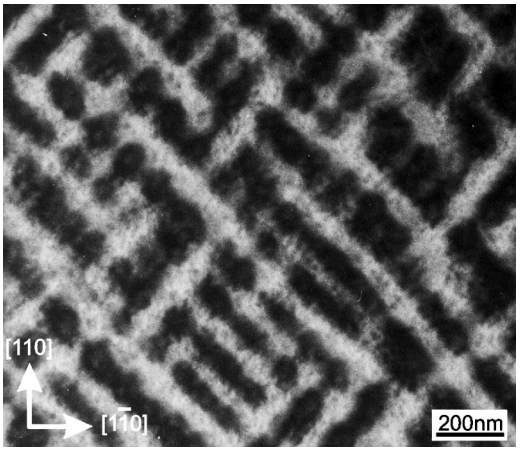

FIG. 4. Many-beam plan-view transmission electron micrograph showing the top-on view of the columnar modulation domains in a 650 °C bulk layer grown on 4° misoriented substrate.

apart from the interface in the middle of the epilayer with nonuniform separation; from $n=0.95$ ML on, it runs through the whole layer. The contrast patterns are not very clearly defined within these micrographs and thus do not provide a reliable measure of the modulation wavelength and the lateral domain size. These would best be estimated from plan-view images, which, however, are not available with the multilayer systems. For a more direct relation to the real size of single domains, the curved contrast contours inside the capping GaAs layers shown by arrows in Figs. 2(d)–2(h) (see also Fig. 2 in Jiang *et al.*[34]) can be used. These contrasts indicate localized elastic distortions due to strain relaxation at the (GaIn)P layer surfaces. It seems interesting to note that there are some indications in Fig. 2(d) of an interference of antiphase boundaries with the modulation structure. In no case were interfacial misfit defects, such as dislocations, observed. For $n>1.7$, the epitaxial growth becomes more and more unstable and the layer quality deteriorates drastically due to the onset of a three-dimensional Stranski-Krastanov growth.[56]

The domain structure of the particular contrast modulation in Fig. 2 has been characterized in detail for $n=1$ growth on 4° off-oriented substrates in a forthcoming paper.[57] There, we have shown by cross-sectional as well as plan-view imaging that two modulation waves running along the [100] and [010] orthogonal directions form columnar domains at the points of intersection. The modulation wavelength was determined from plan-view images to amount to 80 nm, on average. A typical plan-view using many-beam bright-field conditions is shown in Fig. 4 with the 30–50 nm diameter columns seen top-on. This observation finds its counterpart in the ripple topology of an uncapped plan surface of such a strained epilayer when viewed in the atomic force microscope.[57]

Very little information about the structural characteristics of the modulation has come from high-resolution x-ray diffraction (XRD) investigations of bulk layer samples. Weak but noticeable line broadening effects were observed only under inappropriate group-III flux conditions and in layers grown on exactly oriented (001) substrates.[33,55]

Furthermore, we have carried out electron microscopic observations using the compositionally sensitive (002) reflection in cross-sectional dark-field imaging. Contrary to the results reported for InAs/AlAs on InP short-period superlattices,[39,41,42] the contrasts are very blurred with no clear modulation profile being visible. The modulation is visible in $(2\bar{2}0)$ dark field but not as clear as when the $\frac{1}{2}(1\bar{1}1)$ superlattice spot is used.

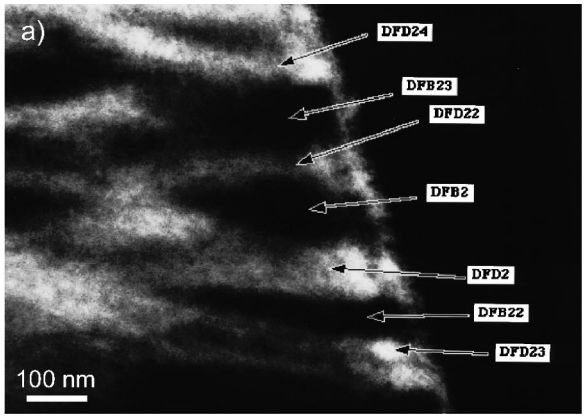

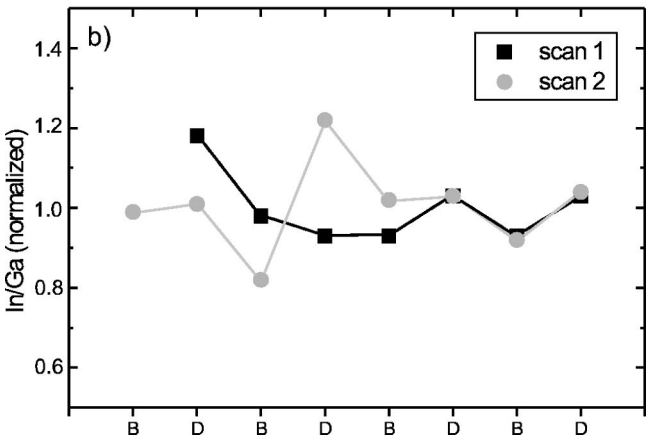

FIG. 5. EDX analyses of the composition variation using a probe width of 10 nm. (a) TEM dark-field image of the modulation in a cross-sectional sample and (b) measured profiles of the In/Ga ratio across domains (*D*) and boundary (*B*) regions.

In order directly to prove the question how far lateral chemical composition variations correlate with the revealed structure modulation, x-ray nanoanalytical techniques were applied, with the knowledge that reliable data are difficult to obtain because of beam broadening effects that deteriorate the attainable spatial resolution and because of the limited detection efficiency. We have taken EDX profiles of layer cross sections parallel to the inner edge of ion-milled samples as shown in Fig. 5(a). For each measurement the focused electron beam was scanned over an area with effective scan width (see Ref. 58) of about 10 nm to ensure sufficient selectivity. Although the lateral extent of a domain boundary is to be assumed considerably small, besides measuring inside contiguous domains also analyses of the intermediate boundary regions were performed. The results of two such runs using the Ga_K and the In_L lines, normalized to an averaged composition of 0.5/0.5 of both components, are summarized in Fig. 5(b). Even though the significance of the variation in the In/Ga ratio is not very high, the experiments may serve as an indication that some phase-separational ef-

fects contribute to the image contrast and have to be taken into account in the discussion of the modulation-formation mechanism.

IV. DISCUSSION

A. Ordering behavior

According to theoretical estimations[3,59] the overall superlattice ordering in (GaIn)P is limited by statistical fluctuations and should remain imperfect even in the best ordered samples. In this paper and others we have established an alternative route to achieve exceptionally high degrees of ordering by the application of a modulated MOVPE growth process. Whereas during continuous growth random intermixing of the alloy constituents provides a natural limitation for ordering, in the modulated epitaxy the individual monolayer thickness of the deposited binary alloys GaP and InP has been proved the determining factor in control of the ordering. The maximum degree of ordering is obtained for a deposition sequence of 1 ML GaP and 1 ML InP.

The early step-terrace reconstruction model[13,14] does not provide a suitable base for an understanding of the above-noted results. The ordering mechanism proposed within the scope of that model consists of an alternate occupation of surface sites by Ga and In as a consequence of a stress minimum principle. Therefore, because of stress minimization, a modulated layer-by-layer growth theoretically should yield the highest degree of ordering at a deposition cycle of $n=0.5$, leading to 1 ML of ordered $Ga_xIn_{1-x}P$. On the other hand, in the view of the step-flow mechanism, this cycling should result in a fractional layer superlattice structure as shown by Fukui and Saito.[60] None of these two cases hold for the observations reported in the present paper.

Our results, however, principally confirm the theoretical surface reconstruction model of Zunger and co-workers.[4,15,20] According to this model, the superlattice ordering during phosphorus-stabilized growth of (GaIn)P can be explained by nearest-neighbor vertical exchange processes of Ga and In atoms within the upper two group-III layers beneath the top phosphorus layer. The driving force for this kind of exchange is provided by the formation of phosphorus dimers and dimer rows at the growing surface and consequently the formation of subsurface compression and tensile stresses. The compressed and dilated lattice sites selectively accommodate atoms according to their respective size.

In Fig. 6 this model is adapted to the scenario of a modulated growth regime for the special case of $n=1$, i.e., 1 ML of GaP and 1 ML of InP, alternately. The sequence of drawings in Figs. 6(a)–6(e) amply illustrates that, in this case, perfect ordering is theoretically achieved when the principles of the reconstruction model of Zunger and co-workers are strictly applied. Experimentally, we found maximum order exactly under the condition of complete covering of the growing surface with one or the other of the two binary species, GaP or InP. It is relatively easy to realize from Fig. 6 that the probability of the incorporation of reconstruction ''faults'' increases with decreasing as well increasing n starting at $n=1$. The alternating deposition of incomplete monolayers at $n<1$ and the deposition of excess atom layers at

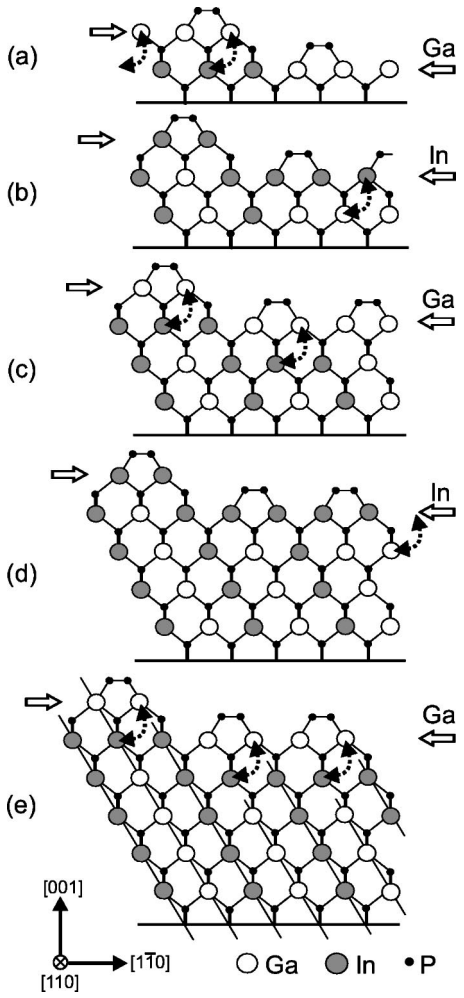

FIG. 6. Schematics of superlattice {111} ordering during reconstruction of a step-containing group-V stabilized surface at alternating deposition of 1 ML of GaP and 1 ML of InP. (a)–(e): Successive deposition cycles and nearest-neighbor vertical group-III atomic exchange processes due to subsurface lattice strains are arrowed. The surface step does not disturb commensuration of the ordering formation.

$n>1$ both introduce occupational disorder into the ordering layers, reducing the global degree of ordering attainable.

The question arises as to the role of surface steps in the reconstruction model. It has been confirmed by a number of continuous-growth epitaxy experiments that the step type (group-III or group-V terminated) and their direction decide about the occurrence and the variant of CuPt-type ordering.[13,14,18,61] It has further been suggested that surface steps are the nucleation sites of antiphase boundaries.[27,62,63] However, quite often commensuration of ordering over distances much larger than the widths of the antiphase domains is observed. The initiation of the surface reconstruction at the step edges and its propagation across the surface treads are the proposed mechanisms to explain such commensurate growth across surface steps on the basis of the step-terrace reconstruction model by Suzuki and Gomyo,[14] and of the vertical-exchange reconstruction model by Philips *et al.*[18] The formation of antiphase boundaries can be attributed to the existence of supersteps formed by step bunching.[63]

Commensuration of the ordering process across steps is also easy to comprehend in light of the modulated layer-by-

layer growth as depicted in Fig. 6. The vertical exchange processes are obviously not disturbed by the presence of a surface step but lead to complete commensuration of ordering across the step. In this work, the substrate misorientation was always a $[1\bar{1}0]$ off-cut producing the $(111)B$ type of steps. In contrast to the results from continuous growth, in many experiments under modulated growth conditions we have found only little influence of different substrate misorientation, i.e., a varying number of steps, on the final degree of ordering.[33,35] These observations support our view of a rather secondary role of steps in the ordering formation.

On the other hand, the mismatch in the ternary system between GaP and GaAs and between InP and GaAs appears to be of considerable importance in the overall structural organization. In continuous growth, this misfit is widely strain-balanced on a macroscopic scale due to random intermixing of both species. During layer-by-layer growth, however, it should increasingly influence the fundamental reconstruction when the elementary layer thickness approaches $n \cong 1$ and higher. Our assertion is that the development of the structural modulation discussed below is an additional reason for the reduction of ordering with increasing monolayer thickness per deposition cycle.

B. Lateral structure modulation

The reversal around $n \cong 1$ in the tendency to order almost coincides with the appearance of the strain-induced modulation pattern that is maintained up to ultimate monolayer thicknesses in the range 1.6–1.7 ML's. Comparable one- and two-directional periodic modulations were reported by several authors for a number of highly strained epitaxial layer systems prepared using MBE and liquid-phase epitaxy techniques.[6,10,11,36–47] Composition variations as large as 15% and more were determined by x-ray microanalysis.[35,42–45] Models have been developed to explain the initiation of morphological and compositional modulations by a nucleation-based strain-induced lateral ordering (SILO) mechanism,[6,11,37,38] by stress-driven step-bunching instabilities,[64] or by considering the elastic deformation and thermodynamic stability of an epitaxial layer surface with atomic size differences and varying lattice parameters of the constituents.[65–67]

The nominal misfit of GaP and InP of approximately $\pm 3.7\%$ with respect to the GaAs substrate creates lateral tensile and compressive strains when matched to GaAs. Usually, under conventional growth conditions and at appropriate growth temperatures and growth rates in the MOVPE of (GaIn)P, coherent heterostructures of even macroscopic dimension are formed with homogeneous strain distribution throughout the epilayers.[57] The same seems true for small n in the modulated-growth regime: The mismatch will partly be accommodated as elastic strain energy and balanced due to the opposite sign of the strain in successive layers, partly compensated by vertical atomic exchange in the upper surface layers. Apparently, when individual layers 0.9 ML thick or more are deposited, it is tempting to suppose an increasing tendency for the growth plane to roughening by coherent aggregation and islanding of the constituent species. During deposition of any new layer, the probablility increases that islands are nucleated by statistical fluctuations and by strain-induced lateral migration of surface atoms. Beyond $n \approx 1$, islanding is inherently connected with the excess adatoms of each binary deposition layer.

Multiple layering of a single binary species due to coherent island formation results in a reduction of the degree of superlattice ordering as discussed in Jiang *et al.*[57] With the vertical atomic exchange becoming increasingly inhibited, also the capability of the epitaxial film to homogeneous accomodation of increasing lateral strain is getting used up. The response of the lattice consists in strain relief by forming a quasiperiodic structure modulation.[8,10,42,66,67] The successive accommodation of islands follows the strain distribution that develops at the vapor-solid interface. This is likely associated with lateral diffusion gradients which additionally force the segregation of the as-deposited group-III atoms. The contribution of strain in the structure formation process is indicated by several microscopic observations, such as the maximum contrast amplitude of the modulaltion in $\frac{1}{2}(1\bar{1}\bar{1})$ rather than in the (002) dark-field, the detection of curved strain contrast contours inside the GaAs intermediate layers, and the observation of a rippling of uncapped plan surfaces by atomic-force microscopy.[57]

Another aspect concerns the relaxational behavior of strained layers when new surfaces are introduced during thin-film preparation as needed for TEM.[42,68,69] The surface relaxation generates lattice distortions by shear strains in the (001) plane (cross-sectional view), and in the $(hk0)$ planes (plan view), so that the electron microscopic thin-sample contrast of the modulation columns also contains diffraction contrast resulting from lattice plane bending due to near-surface relaxation. In our samples, the amplitude of the compositional variation appears rather small as the analytical measurements suggest. Therefore, the image contrast should be less affected by compositional changes, i.e., by direct changes in the atomic scattering factor, than by internal lattice distortions and their near-surface relaxation in the thin-film samples. Final proof of this issue is expected from future analytical x-ray nanoprobe experiments using plan-view samples.

V. SUMMARY

The electron microscopic results obtained in this present work by studying particular double-multilayer samples of (GaIn)P on GaAs provide direct information on the structural evolution during modulated epitaxial growth. The reported quantitative determinations of the degree of $CuPt_B$ superlattice ordering and its change with varying elementary deposition cycle are interpreted in close agreement with current theoretical reconstruction models. They even show aspects of the ordering behavior not yet accounted for by theory. The degree of superlattice ordering derived from electron diffraction analyses as well as from photoluminescence measurements was found to increase until a maximum was reached at layer thicknesses of the individual GaP and InP deposition layers of approximately 1 ML. An opposite trend could be followed when the layer thickness was increased beyond $n \approx 1$. From these observations the conclusion was drawn that the ordering is governed by a growth surface reconstruction in which extensive vertical atomic exchange processes are involved. In contrast to a continuous-growth

method, the alternating layer-by-layer growth leads to the accumulation of the misfit strains between GaP and GaAs and between InP and GaAs with increasing thickness of the individual deposition layers. By this, the strain energy of the system increases until stress relief via structural modulation including possible phase-separational effects becomes more favorable. The modulation is two-dimensional, and the intersection of the two modulation waves creates a columnar domain morphology on a scale less than 80 nm coexisting with the platelike ordered antiphase domains. The progressive modulation increasingly inhibits the ordering formation and becomes the dominating factor in the structural and morphological organization during the epitaxial growth process.

ACKNOWLEDGMENTS

We are greatly indebted to P. Werner, Max-Planck-Institute of Microstructure Physics, Halle, for his collaboration in parts of the electron microscopic work, and to H. Muellejans, Max Planck Institute of Metal Research, Stuttgart, now Institute for Advanced Materials, Petten, The Netherlands, for carrying out the nanoanalytical measurements. Our thanks are also due to T. Suzuki from NEC Corporation, Tsukuba, Japan, for valuable discussions. The work has been supported by the Deutsche Forschungsgemeinschaft (DFG) within the framework of the Collaborative Research Center 383 ''Disorder in Solids on Mesoscopic Scales.''

*Present address: Mechanical and Engineering Department, Louisiana State University, Baton Rouge, LA 70803.

†Email address: ⟨schaper@mailer.uni-marburg.de⟩ Fax: +49 (0) 6421-28 23458

‡Present address: Osram Opto-Semiconductors, 93049 Regensburg, Germany.

[1] S. H. Wei and A. Zunger, Appl. Phys. Lett. **56**, 662 (1990).

[2] D. B. Laks, S. H. Wei, and A. Zunger, Phys. Rev. Lett. **69**, 3766 (1992).

[3] S. H. Wei, D. B. Laks, and A. Zunger, Appl. Phys. Lett. **62**, 1937 (1993).

[4] S. H. Wei and A. Zunger, Phys. Rev. B **49**, 14 337 (1994).

[5] P. Ernst, C. Geng, F. Scholz, H. Schweizer, Y. Zhang, and A. Mascarenhas, Appl. Phys. Lett. **67**, 2347 (1995).

[6] K. Y. Cheng, K. C. Hsieh, and J. N. Baillargeon, Appl. Phys. Lett. **60**, 2892 (1992).

[7] P. J. Pearah, A. C. Chen, A. M. Moy, K. C. Hsieh, and A. Y. Cheng, IEEE J. Quantum Electron. **30**, 608 (1994).

[8] A. G. Cullis, MRS Bull. **21**, 21 (1996).

[9] S. J. Kim, H. Asahi, M. Takemoto, K. Asami, M. Takeuchi, and A. Gonda, Jpn. J. Appl. Phys., Part 1 **35**, 4225 (1996).

[10] Mirecki-Millunchick, R. D. Twesten, S. R. Lee, D. M. Follstaedt, E. D. Jones, S. P. Ahrenkiel, Y. Zhang, H. M. Cheong, and A. Mascarenhas, MRS Bull. **22**, 38 (1997).

[11] H. Asahi, Adv. Mater. **9**, 1019 (1997).

[12] A. Gomyo, T. Suzuki, K. Kobayashi, S. Kawata, I. Hino, and T. Yuasa, Appl. Phys. Lett. **50**, 673 (1987).

[13] T. Suzuki, A. Gomyo, and S. Iijima, J. Cryst. Growth **93**, 396 (1988).

[14] T. Suzuki, and A. Gomyo, J. Cryst. Growth **111**, 353 (1991).

[15] S. Froyen and A. Zunger, Phys. Rev. Lett. **66**, 2132 (1991).

[16] J. E. Bernard, S. Froyen, and A. Zunger, Phys. Rev. B **44**, 11 178 (1991).

[17] A. G. Norman, T.-Y. Seong, B. A. Philips, G. R. Booker, and S. Mahajan, in *Proceedings of the Royal Microscopical Society Conference*, Oxford, 1993, edited by A. G. Cullis, A. E. Staton-Bevan, and J. L. Hutchison, IOP Conf. Proc. Ser. 134 (IOP, Bristol, 1993), p. 279.

[18] B. A. Philips, A. G. Norman, T. Y. Seong, S. Mahajan, G. R. Booker, M. Skowronski, J. P. Harbison, and V. G. Kermidas, J. Cryst. Growth **140**, 249 (1994).

[19] S. B. Zhang, S. Froyen, and A. Zunger, Appl. Phys. Lett. **67**, 3141 (1995).

[20] S. Froyen and A. Zunger, Phys. Rev. B **53**, 4570 (1996).

[21] A. Gomyo, M. Sumino, I. Hino, and T. Suzuki, Jpn. J. Appl. Phys., Part 2 **34**, L469 (1995).

[22] C. S. Baxter, W. M. Stobbs, and J. H. Wilkie, in *Proceedings of the Institute of Physics Conference*, Oxford, 1991, edited by A. G. Cullis and N. J. Long, IOP Conf. Proc. Ser. 117 (IOP, Bristol, 1991), p. 469.

[23] D. S. Cao, E. H. Reihlen, G. S. Chen, A. W. Kimball, and G. B. Stringfellow, J. Cryst. Growth **109**, 279 (1991).

[24] S. R. Kurtz, J. M. Olson, and A. Kibbler, Appl. Phys. Lett. **57**, 1922 (1990).

[25] H. Murata, I. H. Ho, L. C. Su, Y. Hosokawa, and G. B. Stringfellow, J. Appl. Phys. **79**, 6895 (1996).

[26] K. Sinha, A. Mascarenhas, G. S. Horner, R. G. Alonso, K. A. Bertness, and J. M. Olson, Phys. Rev. B **48**, 17 591 (1993).

[27] L. C. Su, I. H. Ho, and G. B. Stringfellow, J. Appl. Phys. **75**, 5135 (1994).

[28] L. C. Su, I. H. Ho, and G. B. Stringfellow, J. Appl. Phys. **76**, 3520 (1994).

[29] P. Bellon, J. P. Chevalier, E. Augarde, J. P. Andre, and G. P. Martin, J. Appl. Phys. **66**, 2388 (1989).

[30] A. Gomyo, S. Kawata, T. Suzuki, S. Iijima, and I. Hino, Jpn. J. Appl. Phys., Part 2 **128**, L1728 (1989).

[31] S. R. Kurtz, J. M. Olson, D. J. Arent, M. H. Bode, and K. A. Bertness, J. Appl. Phys. **75**, 5110 (1994).

[32] H. Murata, I. H. Ho, Y. Hosokawa, and G. B. Stringfellow, Appl. Phys. Lett. **68**, 2237 (1996).

[33] Z. Spika, C. Zimprich, W. Stolz, E. O. Göbel, J. Jiang, A. Schaper, and P. Werner, J. Cryst. Growth **170**, 257 (1997).

[34] J. C. Jiang, A. K. Schaper, Z. Spika, W. Stolz, P. Werner, and L. Tóth, in *Proceedings of the Royal Microscopical Society Conference*, Oxford, 1997, edited by A. G. Cullis and J. L. Hutchinson, IOP Conf. Proc. Ser. 157 (IOP, Bristol, 1997), p. 261.

[35] K. C. Hsieh, J. N. Baillargeon, and K. Y. Cheng, Appl. Phys. Lett. **57**, 2244 (1990).

[36] A. C. Chen, A. M. Moy, P. J. Pearah, K. C. Hsieh, and K. Y. Cheng, Appl. Phys. Lett. **62**, 1359 (1993).

[37] A. C. Chen, A. M. Moy, L. J. Chou, K. C. Hsieh, and K. Y. Cheng, Appl. Phys. Lett. **66**, 2694 (1995).

[38] F. Peiró, A. Cornet, and J. R. Morante, in *Proceeding of the Royal Microscopical Society Conference*, Oxford, 1995, edited by A. G. Cullis and A. E. Staton-Bevan, IOP Conf. Proc. Ser. 146 (IOP, Bristol, 1995), p. 385; Appl. Phys. Lett. **62**, 2265 (1993).

[39] J. Mirecki-Millunchick, R. D. Twesten, D. M. Follstaedt, S. R. Lee, E. D. Jones, Y. Zhang, S. P. Ahrenkiel, and A. Mascarenhas, Appl. Phys. Lett. **70**, 1402 (1997).

[40] A. G. Norman, S. P. Ahrenkiel, H. Moutinho, M. M. Al-Jassim, A. Mascarenhas, J. Mirecki-Millunchick, S. R. Lee, R. D.

Twesten, D. M. Follstaedt, J. L. Reno, and E. D. Jones, Appl. Phys. Lett. **73**, 1844 (1998).
[41] S. P. Ahrenkiel, A. G. Norman, M. M. Al-Jassim, A. Mascarenhas, J. Mirecki-Millunchick, R. D. Twesten, S. R. Lee, D. M. Follstaedt, and E. D. Jones, Appl. Phys. Lett. **84**, 6088 (1998).
[42] R. D. Twesten, D. M. Follstaedt, S. R. Lee, E. D. Jones, J. L. Reno, J. Mirecki-Millunchick, A. G. Norman, S. P. Ahrenkiel, and A. Mascarenhas, Phys. Rev. B **60**, 13 619 (1999).
[43] T. Okada, G. C. Weatherly, and D. W. McComb, J. Appl. Phys. **81**, 2185 (1997).
[44] F. Glas, in *Proceedings of the Royal Microscopical Society Conference*, Oxford, 1993, edited by A. G. Cullis, A. E. Staton-Bevan, and J. L. Hutchison, IOP Conf. Proc. Ser. 134 (IOP, Bristol, 1993), p. 269.
[45] P. Henoc, A. Izrael, M. Quillec, and H. Launois, Appl. Phys. Lett. **40**, 963 (1982).
[46] S. Mahajan, Mater. Sci. Eng., B **30**, 187 (1995).
[47] T. L. McDevitt, S. Mahajan, D. E. Laughlin, W. A. Bonner, and V. G. Keramidas, Phys. Rev. B **45**, 6614 (1992).
[48] D. M. Follstaedt, R. P. Schneider, Jr., and E. D. Jones, J. Appl. Phys. **77**, 3077 (1995).
[49] O. Ueda, M. Takikawa, M. Takechi, J. Komeno, and I. Umebu, J. Cryst. Growth **93**, 418 (1988).
[50] Z. Spika, J. Jiang, C. Zimprich, P. Großmann, A. Schaper, W. Stolz, E. O. Göbel, P. Werner, and J. Feldmann, in *Proceedings of the 23rd International Conference on the Physics of Semiconductors, Berlin*, edited by M. Scheffler, and R. Zimmermann (World Scientific, Singapore, 1996), p. 465.
[51] M. J. Gregor, P. G. Blome, R. G. Ulbrich, P. Grossmann, S. Grosse, J. Feldmann, W. Stolz, E. O. Göbel, D. J. Arent, M. Bode, K. A. Bertness, and J. M. Olson, Appl. Phys. Lett. **67**, 3572 (1995).
[52] C. S. Baxter, R. F. Broom, and W. M. Stobbs, Surf. Sci. **228**, 102 (1990).
[53] J.-P. A. A. Chevalier and A. J. Craven, Philos. Mag. **36**, 67 (1977).
[54] B. T. McDermott, K. G. Reid, N. A. El-Masry, and S. M. Bedair, Appl. Phys. Lett. **56**, 1172 (1990).
[55] Z. Spika, Ph.D. thesis, Philipps University, Marburg, 1997.
[56] D. J. Eaglesham and M. Cerullo, Phys. Rev. Lett. **64**, 1943 (1990).
[57] J. C. Jiang, A. K. Schaper, Z. Spika, and W. Stolz, J. Appl. Phys. **88**, 3341 (2000).
[58] U. Alber, H. Müllejans, and M. Rühle, Ultramicroscopy **69**, 105 (1997).
[59] R. Tycko, G. Dabbagh, S. R. Kurtz, and J. P. Goral, Phys. Rev. B **45**, 134 52 (1992).
[60] T. Fukui, and H. Saito, Appl. Phys. Lett. **50**, 824 (1987).
[61] G. S. Chen and G. B. Stringfellow, Appl. Phys. Lett. **59**, 324 (1991).
[62] M. Ishimaru, S. Matsumura, N. Kuwano, and K. Oki, Phys. Rev. B **51**, 9707 (1995).
[63] G. B. Stringfellow, L. C. Su, Y. E. Strausser, and J. T. Thornton, Appl. Phys. Lett. **66**, 3155 (1995).
[64] J. Tersoff, Phys. Rev. Lett. **77**, 2017 (1996).
[65] B. G. Orr, D. Kessler, C. W. Snyder, and L. Sander, Europhys. Lett. **19**, 33 (1992).
[66] F. Glas, J. Appl. Phys. **62**, 3201 (1987).
[67] F. Glas, Phys. Rev. B **55**, 11 277 (1997).
[68] M. M. J. Treacy, J. M. Gibson, and A. Howie, Philos. Mag. A **51**, 389 (1984).
[69] S. P. Ahrenkiel, in *Electron Crystallography*, edited by D. L. Dorset *et al.* (Kluwer Academic, Dordrecht, The Netherlands, 1997), p. 363.